

Low Damping Differential-Capacitive Sensing Comb

Soon Chang Yeon*, Yun Kwang Jeon*, Yong Hyup Kim **

Department of Aerospace Engineering, College of engineering, Seoul National University,
Shinrim-Dong Kwanak-Ku Seoul 151-742 Korea

*Research assistant, yote@aerojet.snu.ac.kr

** Professor, yhkim@gong.snu.ac.kr

ABSTRACT

Many researchers have proposed high aspect ratio single crystalline silicon structure to improve sensitivity in capacitive sensing for laterally oscillating MEMS devices[1~3]. As the height of structure increases, the capacitive sensing area in high aspect ratio structure is linearly increased while the damping force is cubically increased[4].

In the present study, a specially designed capacitive sensing comb is proposed for low damping and high capacitance characteristics. Geometry of sensing comb is modified to decrease the damping force. Simulations and experiments have been performed with focus on geometrical parameters of the sensing comb.

Keywords: quality factor, squeezed damping, MEMS, high aspect ratio

1 INTRODUCTION

Capacitive displacement sensing method has been widely used in MEMS. The merit of the capacitive sensing comb is simple fabrication process and simple measurement of the displacement. Important factors of the capacitive displacement sensing are area of electrode and distance between moving electrode and fixed electrode. Since area change type senses overlap area change between two electrodes, it has characteristics of relatively small capacitance variation per unit displacement and low damping force. On the other hand distance change type yields large capacitance variation per unit displacement but suffering from high damping force.

Surface micromachined devices prefer distance change type sensing mechanism because large capacitance and damping control with proper inplane shape can be achieved in lateral sensing with low height structure and transverse sensing with etch hole structure[5].

Many researchers have proposed laterally sensing bulk micromachined structures of high aspect ratio single crystalline silicon with large driving and sensing area. However, damping force determining amplitude response and quality factor is significantly increased in high aspect ratio structure. Especially damping force of distance change type cubically increases with height in high aspect ratio

structure. Therefore, high vacuum encapsulation is needed to improve quality factors.

In this paper, we propose new design of sensing comb. It is designed to keep high capacitance change with low damping force. Moreover, it can be made with simple fabrication process. For performance verification of the proposed sensing comb, simulations and experiments have been performed with focus on geometrical parameters of the comb.

2 SQUEEZED DAMPING

Damping of two opposite plates oscillating in the normal direction to the plate is governed by the behavior of fluid between two plates. It is called squeezed damping[4].

In micro scale, inertia effect can be neglected, then the governing equation of fluid is expressed as follows:

$$\frac{\partial}{\partial x} \left\{ \frac{\rho h^3}{\mu} \frac{\partial P}{\partial x} \right\} + \frac{\partial}{\partial y} \left\{ \frac{\rho h^3}{\mu} \frac{\partial P}{\partial y} \right\} = 12 \frac{\partial(\rho h)}{\partial t} \quad (1)$$

where ρ is density, h is fluid thickness, μ is viscosity, P is pressure of fluid.

Equation (1) is simplified by applying the assumption of isothermal, small pressure variation and small displacement as follows:

$$\frac{\partial P^*}{\partial x^2} + \frac{\partial P^*}{\partial y^2} = 12 \frac{\mu}{h_o^3} \frac{\partial h}{\partial t} \quad (2)$$

where P^* is the pressure departure within the fluid from the ambient value, h_o is the initial fluid thickness. Rectangular plate damping force can be obtained by integrating the solution of Eqn.(2). For a rectangular plate of width W , length L , $h_o = \text{const}$ and equivalent velocity of the plate, the damping force is expressed as follows:

$$F_D = B_{\text{squeez}} v = \mu c_f \frac{W^3 L}{h_o^3} \frac{\partial h}{\partial t} \quad (L > W) \quad (3)$$

where B_{squeez} is squeezed damping coefficient, v is velocity of the plate, and c_f is rectangular shape coefficient.

3 SENSING COMB DESIGN

In this section, we investigate the design parameter from the analytic solution for low damping and high capacitive

sensing comb which can be fabricated with simple bulk micromachining process. In sensing comb design, we focus on simplicity of fabrication process, minimization of damping coefficient without deteriorating capacitance variation per unit displacement.

In Eqn. (3) squeezed damping coefficient is proportional to a longer side of the plate, and the cube of a shorter side. Therefore, the damping coefficient is dominated by the dimension of a shorter side of the plate, which will be called effective width in this study.

Inplane geometry of Surface micromachined device oscillating in normal direction to substrate can be easily changed with etch hole, shape change and etc. Therefore, damping force can be controlled with effective width in Eqn. (3)[5]. In case of laterally oscillating surface micromachined structure, the damping coefficient is not relatively large, because effective width W (height of the structure) in Eqn. (3) is usually very small. However, the damping coefficient of bulk micromachined laterally oscillating structure is much larger than the surface micromachined structure, because effective width (height of structure) is often several dozens of micrometer.

Capacitance of rectangular plate can be expressed as

$$C \propto \frac{WL}{h_o} \quad (4)$$

Note that the damping coefficient is proportional to the cube of effective width while the capacitance is linearly proportional to it as shown in Eqn. (3) and (4).

Our design key is to separate the sensing comb into several divisions while maintaining the total sensing area same. This design leads to the sensing comb with reduced damping coefficient while keeping the magnitude of capacitance variation.

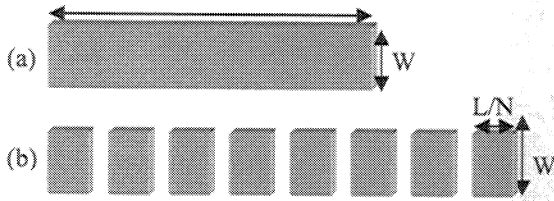


Fig. 1. Same total area rectangular plate with different sub area

The squeezed damping coefficient of plates which have same total area in Fig. 1 is

$$\begin{aligned} B_{(a)} &\propto \frac{W^3 L}{h_o^3} & L > W \\ B_{(b)} &\propto N \times \frac{(L/N)^3 W}{h_o^3} = \frac{W^3 L}{N^2 h_o^3} & \frac{L}{N} < W \\ B_{(a)} &\gg B_{(b)} \end{aligned} \quad (5)$$

where N is the number of divisions of the comb. Equation (5) implies that if sub plate length is smaller than the height of structure, the damping coefficient can be reduced.

Fig. 2 illustrates the proposed sensing comb. The differential capacitive sensing comb type is adopted for design. It consists of two parts; rotor (moving electrode) and two stator (fixed electrode). Stators are separated into several divisions and each division is supported by individual anchor.

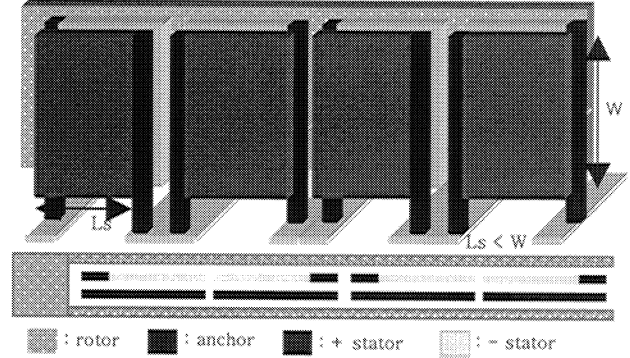


Fig. 2. Illustration of designed sensing comb

4 SIMULATION

To prove efficiency of the present comb, analytical simulation has been performed with a proper assumption. More precise results can be obtained with the numerical simulation such as finite element method.

4.1 Analytic Simulation

The closed form expression of damping coefficient can be obtained with assumption that pressure departure is zero at the stator boundary.

From the Eqn. (3), the damping coefficient between rotor and stator is expressed as:

$$B_{stator} = N \times \mu c_{fs} \frac{L_s^3 W}{d_c^3} \quad (L_s < W) \quad (6)$$

where N is the number of stators, W is the height of structure, d_c is the thickness of the fluid film between stator and rotor, c_{fs} is the geometry coefficient of the stator and L_s is the width of the stator. The damping coefficient between rotors is expressed as:

$$B_{gab} = N \times \mu c_{fg} \frac{L_g^3 W}{d_g^3} \quad (7)$$

where c_{fg} is the geometry coefficient of the gap, d_g is the fluid film thickness between rotors and L_g is the width of the gap. The total damping coefficient of the sensing comb is summation of Eqn. (6) and (7)

$$B_{stator} + B_{gab} = \mu W N \times \left(c_{fs} \frac{L_s^3}{d_c^3} + c_{fg} \frac{L_g^3}{d_g^3} \right) \quad (8)$$

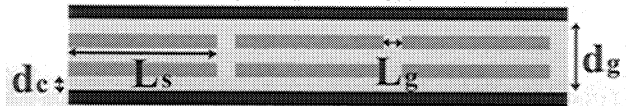


Fig. 3. Geometric parameters of designed comb

4.2 Numerical Analysis

Numerical analysis with ANSYS(finite element method) has been performed for more precise simulation. Many researchers have investigated the squeezed film damping analysis with existing finite element thermal analysis for complex plate shape and velocity gradient[4~6].

More accurate boundary condition is available in numerical analysis. Squeezed film has zero pressure departure boundary condition along the plate edge which is rotor in present sensing comb. This boundary condition can't be easily applied in analytic simulation, because film thickness not uniform in present sensing comb.

The governing equation of thermal conductivity is expressed as follows:

$$\frac{\partial}{\partial x} \left\{ k \frac{\partial T}{\partial x} \right\} + \frac{\partial}{\partial y} \left\{ k \frac{\partial T}{\partial y} \right\} + \dot{q} = \rho c_p \frac{\partial T}{\partial t} \quad (9)$$

The thermal conductivity equation has same form as the governing equation of fluid in Eqn. (1) if variables are replaced as follows:

$$T = P^*, k = \frac{\rho h_o^3}{\mu}, \dot{q} = -12 \frac{\partial(\rho h)}{\partial t}, c_p = 0 \quad (10)$$

Then the squeezed damping problem with complex geometry, velocity and fluid film thickness can be solved with Eqn. (9) and (10).

4.3 Result

The damping coefficients of the conventional comb and the present comb have been solved analytically as well as numerically and are plotted in Fig. 4. The conventional comb has length of $200\mu\text{m}$ and the fluid thickness between stator and rotor is $2\mu\text{m}$. In the present comb the stator is separated into 10 divisions without changing the total area. Therefore, each stator of the present comb has the length of $20\mu\text{m}$ and the fluid thickness is same as the conventional comb. As shown in the figure, damping coefficient of the present comb is greatly reduced compared to the conventional comb. The damping coefficient obtained from the analytic simulation is evaluated lower than the numerical analysis and the difference between two approaches becomes longer as the height of the comb increases. The underestimation of the damping coefficient in the analytic simulation is due to the assumption of zero pressure departure boundary condition along the stator edge. Note that the damping coefficient of the conventional comb varies cubically while the present comb has linear variation of the damping coefficient, which agree with Eqn. (3). It is because the height of the comb is shorter than the length in the conventional comb while it is longer than the length in the present comb.

Figure 5 shows the damping coefficient variation with respect to the length of the stator(Effective width) in the present comb. As the effective width increases, the damping coefficient increases, too. However, the damping coefficient of the present comb is much lower than the conventional comb.

Figure 6 shows the pressure departure distribution of present comb with several divisions of stator. Small amount of pressure departure within the gap changes the pressure departure along the stator boundary edges, and leads to the change of pressure departure distribution over the stator. Note that the pressure departure distributions on the stator located at both ends are quite different from those on the inside stator, which is due to the zero pressure departure boundary condition along the both ends.

As shown in Fig. 7, as the gap width increases, the pressure departure of the gap decreases, and therefore, numerical solution comes close to the analytic solution with zero pressure departure boundary condition.

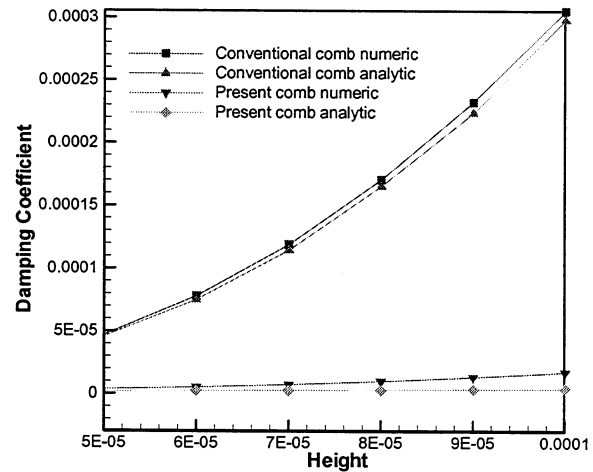


Fig. 4. Damping coeff. of present comb and conventional comb

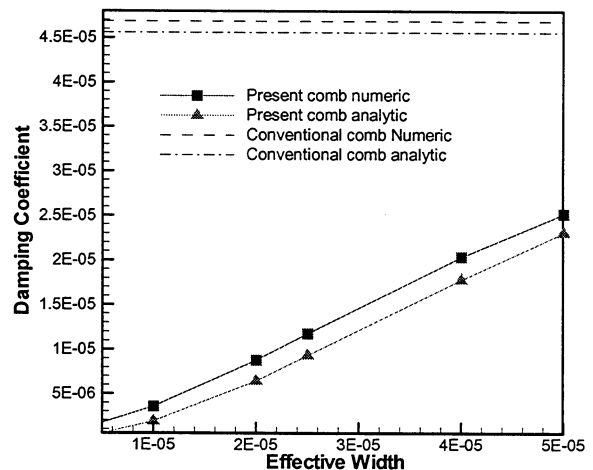


Fig. 5. Damping coeff. of present comb with stator length

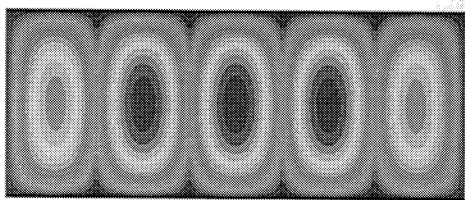


Fig. 6. Pressure departure distribution of designed comb

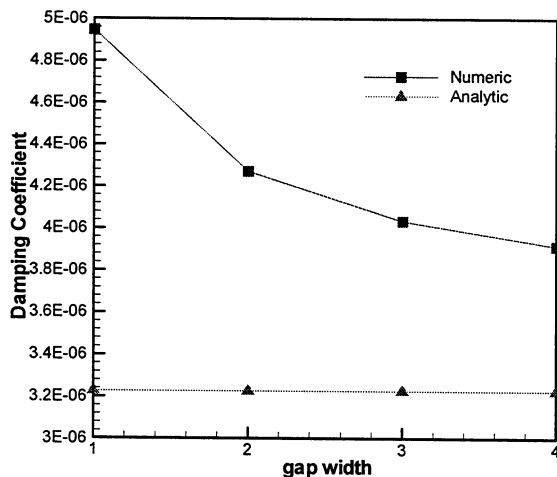


Fig. 7. Gap width effect of present comb

5 FABRICATION

The capacitive displacement sensing comb is fabricated using bulk micromachining with single crystalline silicon. Figure 8 shows the fabrication process flow of the present comb. A glass wafer is used to make electrical isolation between the proof mass and electrode. Anchor and gold electrode is pre-defined on the silicon and glass wafer, respectively. Glass wafer is coated with 1000Å Au using sputtering, and then patterned. The Au layer works as electrode as well as intermediate layer for eutectic bonding. Backside of silicon wafer is patterned by Deep RIE to 10μm deep using PR mask. This pattern works as an anchor which supports the structure on the glass wafer. The patterned silicon and glass wafers are precisely align bonded together using eutectic bonding. Anchor pattern should be bonded strongly on the Au electrode pattern. Silicon side of bonded wafer is etched in KOH to get desired structure height.(about 60μm) On account of the high roughness of lapped silicon surface, chemical mechanical polishing(CMP) process should be performed. CMP process makes silicon structure height to 50μm. On the silicon surface, Silicon oxide of etch mask is deposited to 3000Å and patterned in RIE. Finally silicon is etched to the bottom using Deep RIE for comb structure.

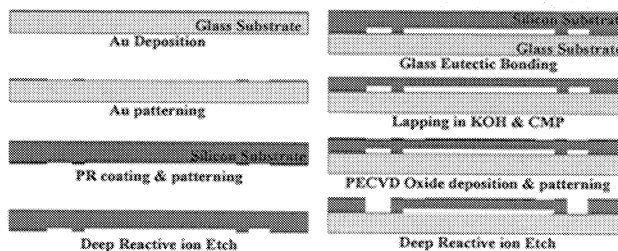


Fig. 8. Fabrication Process

6 CONCLUSION

Low damping and high capacitive displacement sensing comb is proposed with simple bulk micromachining process. The performance of the present comb has been estimated by analytical and numerical simulations. The sensing comb is fabricated and the performance is measured to demonstrate the efficiency of the present comb.

The proposed sensing comb is effective for displacement measurement especially in structure with high aspect ratio such as bulk micromachined laterally oscillating devices.

REFERENCE

- [1] Hiroshi Kawai, 'High resolution micro gyroscope using vibratory motion adjustment technology', Sensors and Actuators A, vol. 90, 2001, pp.153-159
- [2] Seong-Hyok Kim, June-Young Lee, Che-Heung Kim and Yong-Kweon Kim, The 11th International conference on Solid state Sensors and Actuators, June, 2001, pp.476-479.
- [3] Jason W. Weigold, khalil Najafi, Stella W. Pang "Design and fabrication of Submicrometer, Single crystal Si accelerometer" IEEE Journal of MEMS Vol.10, No. 4, pp 518-524, 2001.
- [4] James B. Starr "Squeeze Film Damping in Solid State Accelerometers." Technical Digest IEEE Solid State Sensor and Actuator Workshop, pp 44-47, June 1990
- [5] Eung-Sam Kim, Young-Ho Cho and Moon-Uhn Kim, "Effect of Holes and Edges on the Squeeze film damping of perforated micromechanical structures", IEEE, 1999, pp. 296-301
- [6] Gabriele Schrag, Gerhard Wachutka, " Physically based modeling of squeeze film damping by mixed-level system simulation", Sensors and Actuators A, 97-98, 2002, pp.193-200